

Nonadiabatic Molecular Dynamics Simulations of Correlated Electrons in Solution. 2. A Prediction for the Observation of Hydrated Dielectrons with Pump–Probe Spectroscopy

Ross E. Larsen and Benjamin J. Schwartz*

Department of Chemistry and Biochemistry, University of California, Los Angeles, California 90095-1569

Received: September 19, 2005; In Final Form: October 25, 2005

The hydrated dielectron is a highly correlated, two-electron, solvent-supported state consisting of two spin-paired electrons confined to a single cavity in liquid water. Although dielectrons have been predicted to exist theoretically and have been used to explain the lack of ionic strength effect in the bimolecular reaction kinetics of hydrated electrons, they have not yet been observed directly. In this paper, we use the extensive nonadiabatic mixed quantum/classical excited-state molecular dynamics simulations from the previous paper to calculate the transient spectroscopy of hydrated dielectrons. Because our simulations use full configuration interaction (CI) to determine the ground and excited state two-electron wave functions at every instant, our nonequilibrium simulations allow us to compute the absorption, stimulated emission (SE), and bleach spectroscopic signals of both singlet and triplet dielectrons following excitation by ultraviolet light. Excited singlet dielectrons are predicted to display strong SE in the mid infrared and a transient absorption in the near-infrared. The near-infrared transient absorption of the singlet dielectron, which occurs near the peak of the (single) hydrated electron's equilibrium absorption, arises because the two electrons tend to separate in the excited state. In contrast, excitation of the hydrated electron gives a bleach signal in this wavelength region. Thus, our calculations suggest a clear pump–probe spectroscopic signature that may be used in the laboratory to distinguish hydrated singlet dielectrons from hydrated electrons: By choosing an excitation energy that is to the blue of the peak of the hydrated electron's absorption spectrum and probing near the maximum of the single electron's absorption, the single electron's transient bleach signal should shrink or even turn into a net absorption as sample conditions are varied to produce more dielectrons.

I. Introduction

In the previous paper, henceforth called Paper I, we reported in detail the results of extensive computer simulations of the excited-state relaxation dynamics of hydrated dielectrons.¹ Hydrated dielectrons, which are predicted to consist of two paired electrons confined to a single cavity in liquid water,^{2–5} are of theoretical interest because they are an example of a solvent-supported state whose properties are influenced strongly by electron correlation.^{1,5} Experimentally, hydrated dielectrons have garnered interest because of the role they may play in solution-phase radiation chemistry.^{6,7} Despite this theoretical and experimental interest, however, hydrated dielectrons have not been observed directly. Early reports of the direct spectroscopic observation of hydrated dielectrons⁸ have been dismissed as artifacts by some,⁹ although the presence of dielectrons has been used to explain the curious lack of an ionic strength effect in the bimolecular recombination of (single) hydrated electrons.⁷

One reason that dielectrons may have not been observed directly is that it is not clear what experiment would unequivocally identify them. The difficulty lies in the fact that it is impossible to create hydrated dielectrons without also making large numbers of (single) hydrated electrons, and the presence of large numbers of hydrated electrons could mask the spectral signatures of dielectrons. Figure 1 shows the calculated equilibrium absorption spectra of singlet (dashed curve) and triplet (dotted curve) hydrated dielectrons, along with the absorption spectrum of the hydrated electron (solid curve); we have discussed the features of these absorption spectra in detail in previous work.⁵ The figure makes it clear that dielectrons of

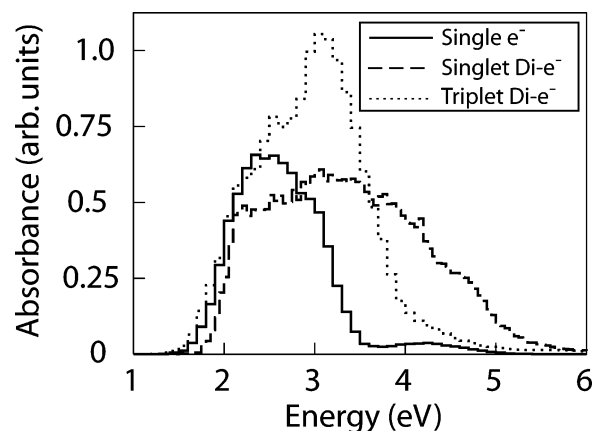


Figure 1. Calculated equilibrium absorption spectra of the hydrated electron (solid curve), singlet hydrated dielectron (dashed curve), and triplet hydrated dielectron (dotted curve). The spectrum for the (single) hydrated electron was computed from the lowest 10 adiabatic eigenstates taken from a 20 ps adiabatic, ground-state simulation with the same electron–water pseudopotential used in the dielectron simulations described in the text and in Paper I.¹ The spectra for the singlet and triplet hydrated dielectrons were calculated from the 30 ps adiabatic ground-state simulations described in ref 5.

either spin absorb strongly to the blue of the hydrated electron, so that one potential method for observing dielectrons spectroscopically would be to search for a nonlinear increase in absorption at a blue wavelength (e.g., at 4.0 eV)¹⁰ as the concentration of hydrated electrons is systematically increased. This approach to detecting dielectrons would be quite challeng-

ing, however, because the production of hydrated electrons by multiphoton ionization is itself nonlinear, so that this type of search for dielectrons involves detangling two competing nonlinear effects. In this paper, we use the full configuration interaction (CI), nonadiabatic, mixed quantum/classical molecular dynamics simulations described in Paper I to calculate the pump–probe signature of hydrated dielectrons. We demonstrate that singlet dielectrons indeed have a pump–probe spectroscopic signature that is distinct from that of hydrated electrons and suggest an experiment that uses specific pump and probe wavelengths to maximize the chances to detect hydrated dielectrons spectroscopically.

The rest of this paper is organized as follows. Section II describes the methods used to compute the transient pump–probe spectroscopy of excited dielectrons. Section III presents the results of these calculations for both singlet and triplet dielectrons and compares their transient spectroscopy to that of the hydrated electron. This allows us to present a prediction for the spectroscopic observation of hydrated dielectrons in the presence of large numbers of hydrated electrons. We propose that one should optically pump a sample containing both electrons and dielectrons well to the blue of the peak of the hydrated electron’s absorption spectrum and probe at a wavelength near the electron’s absorption maximum. Our prediction is that for this combination of pump and probe wavelengths, hydrated electrons give a transient bleach whereas dielectrons are predicted to give a transient absorption. Thus, the presence of dielectrons would be clearly indicated by a change in sign of the transient spectroscopic signals. Section IV discusses these results and comments on the prospects of experimentally verifying the existence of hydrated dielectrons.

II. Methods for Calculating the Pump–Probe Transient Spectroscopy of Hydrated Dielectrons

In this section, we outline how we use the nonequilibrium, excited-state trajectories discussed in Paper I to calculate the pump–probe spectroscopy of both singlet and triplet hydrated dielectrons. The methods used for the full CI nonadiabatic calculations are described in Paper I, and we refer the reader there for more details.¹ In brief, for both singlet and triplet dielectrons, we have run 30 nonequilibrium, constant–energy mixed quantum/classical (QM/CM) molecular dynamics simulations at a temperature of ~ 300 K. The simulations were performed in a cubic box 18.17 \AA on a side that contains 200 classical water molecules and two excess electrons; all interactions were computed using minimum-image periodic boundary conditions¹¹ with the interactions tapered smoothly to zero at half the box length.¹² The classical water motions were propagated using the velocity Verlet algorithm with a time step of 0.5 fs, with the inter- and intramolecular interactions of the water given by the SPC/Flex potential.¹³ The two excess electrons repel each other through the Coulomb interaction, and they interact with the solvent molecules through a pairwise pseudopotential introduced by Schnitker and Rossky.¹⁴ For each water configuration, we compute the adiabatic two-electron eigenstates of the system using full configuration interaction (CI), as described briefly in Paper I and in greater detail in refs 4 and 5. The nonadiabatic dynamics of the two–electron system were calculated using Prezhdo and Rossky’s mean-field with surface hopping (MF/SH) algorithm.¹⁵

Our methodology to compute the pump–probe transient spectra is essentially the same as that used previously by Schwartz and Rossky for the hydrated electron.¹⁶ For each of the 30 nonequilibrium trajectories, which we denote by $I = 1,$

2, ..., 30, we resonantly excite the system by $4.00 \pm 0.01 \text{ eV}$ to an adiabatic (di)electronic state, $|\Psi_{\text{exc}}\rangle$, at time $t = 0$. For each excited–state trajectory, the time-resolved change in absorbance, in the limit of inhomogeneous broadening, is a sum of transient absorption and stimulated emission (SE) components, which we denote $A_I(t; E)$ and $S_I(t; E)$, respectively,

$$A_I(t; E) \propto \sum_{i=\min}^{N(N\pm 1)/2} \frac{|\langle \Psi_i | \mathbf{P} | \Psi_{\text{MF}} \rangle|^2}{(E_i - E_{\text{MF}})} \delta(E - (E_i - E_{\text{MF}})) \quad (1)$$

$$S_I(t; E) \propto \sum_{i=1}^{\min-1} \frac{|\langle \Psi_i | \mathbf{P} | \Psi_{\text{MF}} \rangle|^2}{(E_{\text{MF}} - E_i)} \delta(E - (E_{\text{MF}} - E_i)) \quad (2)$$

where $\mathbf{P} = \mathbf{p}_1 + \mathbf{p}_2$ is the two-electron momentum vector operator (see ref 5), MF denotes the mean-field state of the system, *min* represents the lowest-lying adiabatic state for which $E_{\min} - E_{\text{MF}} > 0$, and the adiabatic wave functions and energies are evaluated at time t after excitation.¹⁷ In addition, the experimentally observable signal also includes contributions from the ground-state bleach, which is the absorption from the ground state that is *missing* due to the excitation,

$$B_I(t, E) \propto \sum_{i=2}^{N(N\pm 1)/2} \frac{|\langle \Psi_i | \mathbf{P} | \Psi_1 \rangle|^2}{(E_i - E_1)} \delta(E - (E_i - E_1)) \quad (3)$$

with the same notation as for eqs 1 and 2, except that the energies and wave functions in eq 3 are from configurations generated by dynamics with the dielectron in its two–electron ground state and started from the same initial conditions as excited state run I .

We have defined the SE and bleach components in eqs 2 and 3, respectively, as being positive definite, but experimentally SE and bleaching yield a *decrease* in optical density. Thus, for each nonequilibrium trajectory, I , the total change in absorption is

$$\Delta OD_I(t; E) \propto A_I(t; E) - S_I(t; E) - B_I(t; E) \quad (4)$$

and therefore we display $-S$ and $-B$ below in Figures 2 and 4. Since the initial configuration in each excited-state trajectory had a different probability of absorbing the $\sim 4\text{-eV}$ excitation photon, we weighted each trajectory in the nonequilibrium ensemble by $|\langle \Psi_{\text{exc}} | \mathbf{P} | \Psi_1 \rangle|^2 / (E_{\text{exc}} - E_1)$ evaluated at time $t = 0$, so the ensemble-averaged change in absorption is

$$\langle \Delta OD(t; E) \rangle \propto \sum_I \frac{|\langle \Psi_{\text{exc}} | \mathbf{P} | \Psi_1 \rangle|^2}{(E_{\text{exc}} - E_1)} \Delta OD_I(t; E) \quad (5)$$

The same type of weighting also defines the nonequilibrium averages for the individual SE, absorption, and bleach component spectra, $\langle S(t; E) \rangle$, $\langle A(t; E) \rangle$, and $\langle B(t; E) \rangle$, respectively. We note that the Condon approximation was found to hold for the computed spectroscopy of the hydrated electron, i.e., that $|\langle \Psi_{\text{exc}} | \mathbf{P} | \Psi_1 \rangle|^2 / (E_{\text{exc}} - E_1)$ is the same for all initial configurations.¹⁶ For both singlet and triplet dielectrons, however, these initial weights varied significantly for different configurations (i.e., the Condon approximation fails), so the absorption cross section was kept inside the sum, as written explicitly in eq 5.

For each component of the transient spectroscopy, we computed the frequency dependence by placing the energy-weighted transition dipoles into 0.2 eV wide bins for the singlet dielectron spectra and 0.1 eV wide bins for the triplet dielectron

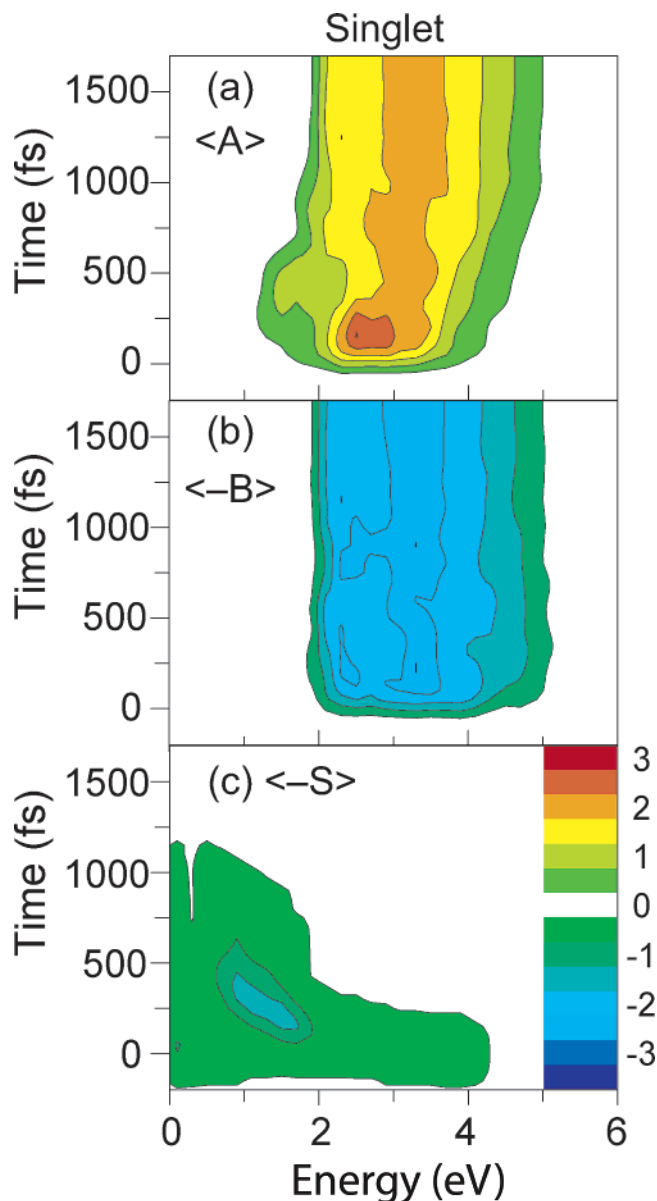


Figure 2. Ensemble-averaged transient spectral components of the singlet dielectron, calculated as described in the text. Panel A: Absorption spectrum, $\langle A(t; E) \rangle$ (eq 1), computed from the 30 excited-state trajectories. Panel B: Negative of the ground-state bleach, $\langle -B(t; E) \rangle$ (eq 3), computed from the same initial configurations as the absorption but using the ground-state trajectory. Panel C: Negative of the stimulated emission, $\langle -S(t; E) \rangle$ (eq 2), computed from the 30 excited-state trajectories. Note that the bleach and SE components give negative changes in optical density, so that the total spectrum, eq 4, may be found directly as the sum of panels A–C. The spectra are reported in arbitrary units, but with the same color scale (shown in panel B) for all three panels.

spectra. We chose the bin widths to be the narrowest possible without an unacceptable level of noise; since the triplet spectrum is narrower than the singlet, we were able to use narrower bins for the triplet spectra. The transition dipoles and energies were calculated every 3 fs for both the excited-state (absorption and stimulated emission) and ground-state (bleach) runs. The spectral dynamics were then convolved in time with a Gaussian having a full width at half-maximum of 150 fs, corresponding to the instrument response for the ultrafast spectroscopic measurements performed in our laboratory.¹⁸ Finally, the runs were terminated after the transient dynamics had returned to equilibrium, typically within 200–500 fs of reaching the ground state. Thus,

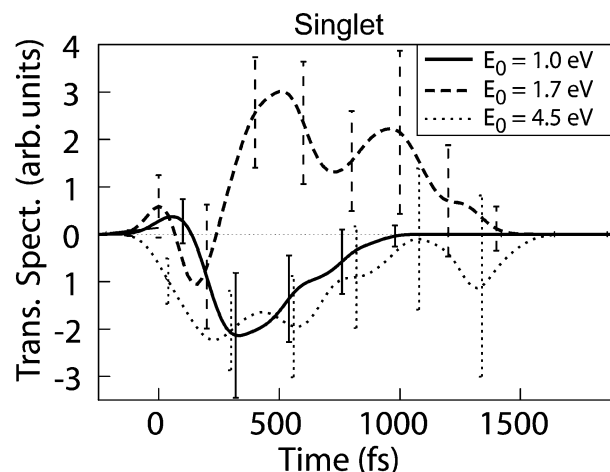


Figure 3. Single-frequency cuts of the total transient absorption spectrum of the hydrated singlet dielectron, eq 4, computed as $\int^{E_0+\Delta E}_{E_0-\Delta E} dE \langle \Delta OD(t; E) \rangle$, with $\Delta E = 0.1$ eV for $E_0 = 1.0$ eV (solid curve), $E_0 = 1.7$ eV (dashed curve), and $E_0 = 4.5$ eV (dotted curve). The curves are convolved with a 150 fs full width at half-maximum Gaussian response function, and the error bars are plus or minus one standard deviation.

for the times after each trajectory had ended, we assumed that the transient absorption component, A_t , was the same as the equilibrium dielectron absorption spectrum.

We conclude this section by noting that although it is more convenient analytically to write the transition strength between our CI eigenstates in terms of the momentum operator, for the numerical computations presented here we proceeded as described in ref 5. Briefly, in our implementation of CI for dielectrons,⁴ we expanded the adiabatic wave functions in terms of appropriately antisymmetrized products of single-electron adiabatic eigenstates,

$$|\Psi_i\rangle = \sum_{n,m} c_{n,m}^{i,\pm} |n,m\rangle_{\pm} \quad (6)$$

where $|n,m\rangle_{\pm} = (|n\rangle_1|m\rangle_2 \pm |m\rangle_1|n\rangle_2)/\sqrt{2}$, $|n,n\rangle_+ = |n\rangle_1|n\rangle_2$, and $|n\rangle_k$ denotes a single electron eigenstate for electron k ; the plus sign denotes spin singlet dielectrons and the minus sign triplet dielectrons, with $m \geq n$ for the singlet and $m > n$ for the triplet case. To calculate the necessary transition dipoles, we inserted eq 6 into eqs 1–3, expanded the products, and replaced the single-electron momentum operators with position operators using the well-known single-electron operator identity $\langle k|\mathbf{p}|n\rangle = im\omega_{kn}\langle k|\mathbf{r}|n\rangle$, where m is the mass of the electron, $\omega_{kn} = (\epsilon_k - \epsilon_n)/\hbar$, and ϵ_k, ϵ_n are the single-electron eigenenergies of single-electron states k and n , respectively.¹⁷

III. Results

A. Transient Spectroscopy of the Excited Singlet Hydrated Dielectron. Figure 2 displays contour plots of each component of the nonequilibrium ensemble-averaged transient spectroscopy of the hydrated singlet dielectron. Panel A shows the transient absorption spectrum, $\langle A(t; E) \rangle$. The excited-state absorption spectrum initially has a peak at ~ 2.8 eV and is roughly 2 eV wide. During the first 700 fs, this absorption shifts to the blue and broadens slightly because the gap between the energy of the occupied excited state and higher lying excited states increases, which results from the fact that solvation causes the two electrons to partially dissociate in the excited state (see Figures 1 and 3 of Paper I). As the excited trajectories reach the ground state and reequilibrate, the transient absorption

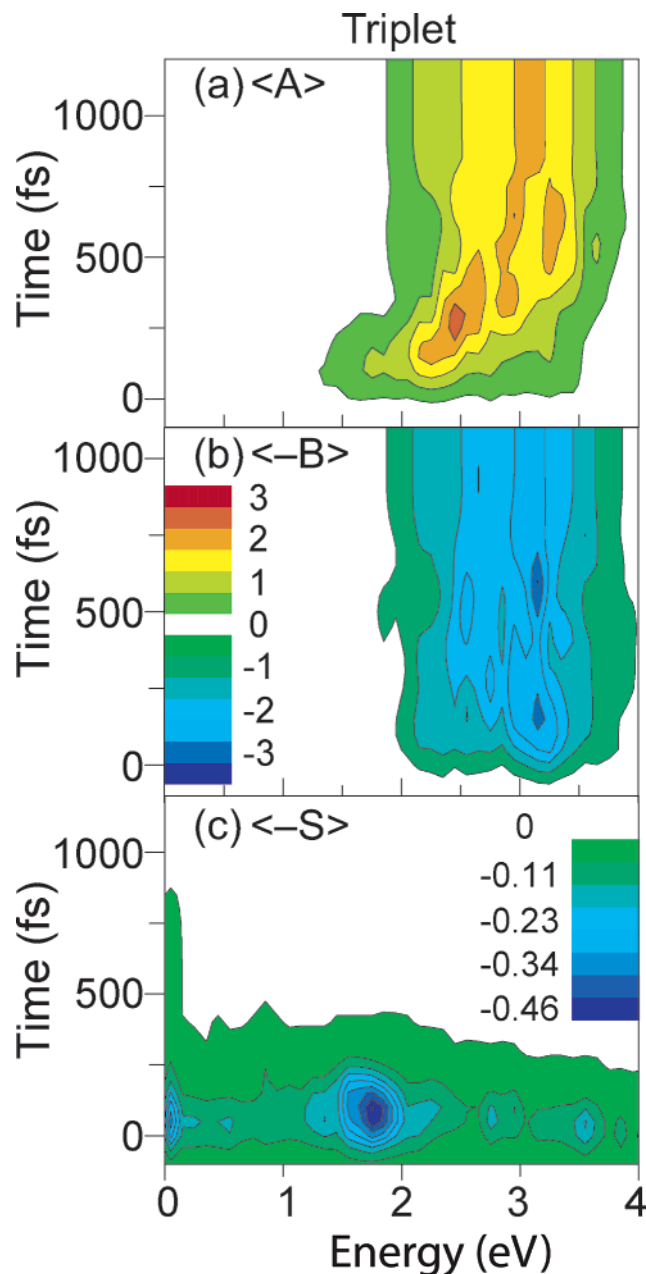


Figure 4. Ensemble-averaged transient spectral components of the triplet dielectron, calculated as described in the text. Panel A: Absorption spectrum, $\langle A(t; E) \rangle$ (eq 1), computed from the 30 excited-state trajectories. Panel B: Negative of the ground-state bleach, $\langle -B(t; E) \rangle$ (eq 2), computed from the same initial configurations as the absorption but using the ground-state trajectory. Panel C: Negative of the stimulated emission, $\langle -S(t; E) \rangle$ (eq 2), computed from the 30 excited-state trajectories. Note that the bleach and SE components give negative changes in optical density, so that the total spectrum, eq 4, may be found directly from the sum of panels A–C. The spectra are reported in arbitrary units, with the same color scale (shown in panel B) for panels A and B; the range of values displayed in panel C differs from that in panels A and B, but the scale is the same as for the upper two panels.

spectrum approaches the equilibrium ground state absorption spectrum (cf. Figure 1). Panel B shows the ground-state bleach, $\langle -B(t; E) \rangle$, which looks essentially like the equilibrium absorption spectrum convolved with the instrument response for all times greater than zero. The fact that there is little dynamics in the ground-state bleach is not surprising, given that the absorption spectrum is a superposition of transitions to nearly a dozen states, so that removal of the ground-

state burns the entire electronic progression, creating “replica holes” that mask any spectral diffusion.^{19,20} In addition to the transient absorption and bleach components, the excited singlet dielectron also shows a significant transient SE, $\langle -S(t; E) \rangle$, shown in Panel C. Immediately after excitation, the singlet dielectron has a broad SE at all energies less than the excitation energy of ~ 4 eV. The small amplitude to the blue of 4 eV is caused by inertial fluctuations that increase the ground-to-occupied-state energy gap before relaxation has time to occur. As time elapses, the energy of the excited dielectron decreases due to nonadiabatic relaxation and the energy of the unoccupied ground state increases due to solvation (see Figure 2 of Paper I¹), so by the time only the first excited state is populated, the SE spectrum has red-shifted and narrowed. The net result is a strong SE component centered at ~ 1 eV that begins at ~ 150 fs and lasts for ~ 300 fs, with weaker SE continuing until $t \sim 1$ ps, after which not enough trajectories remain excited to show appreciable SE.

Since the excited-state absorption in Panel A begins with significant absorption to the red of the ground-state bleach and a deficit of absorption to the blue of the ground-state bleach, in the total transient spectroscopy we expect to see a net transient bleach lasting ~ 700 fs at probe energies greater than ~ 4 eV and an equally long-lived net transient absorption at probe energies less than ~ 2 eV. The SE also overlaps with the excited-state absorption for the first ~ 500 fs, so some of the net transient absorption to the red of the equilibrium spectrum is partially canceled. In fact, given the statistical error of the simulations, we have found that contour plots of the full transient absorption spectrum, $\langle \Delta OD \rangle$, are quite noisy due to cancellations between the different components of the signal. In Figure 3, therefore, we display only cuts of the total spectroscopy at selected frequency ranges that have appreciable net signal beyond the simulation noise. The low-frequency oscillations seen in all of the cuts are associated with low-frequency solvent motions and are artifacts of our finite statistics; with a larger number of excited-state runs, we expect these oscillations to disappear.¹⁶ At low energies, ~ 1 eV, there is substantial SE that takes several hundred femtoseconds to appear and decays in less than 1 ps. This growth and decay of the SE tracks the formation of a quasi-equilibrated first excited state consisting of two lobes of charge in a single cavity (see Figure 3 of Paper I¹) and its subsequent decay by nonadiabatic transition.

B. Transient Spectroscopy of the Excited Triplet Hydrated Dielectron. Figure 4 displays contour plots of the ensemble-averaged components of the transient spectroscopy of the photoexcited triplet hydrated dielectron. Panel A shows the transient absorption spectrum, $\langle A(t; E) \rangle$, which begins with a strong absorption at energies ~ 2.8 eV that shifts rapidly to the blue because a gap opens between the occupied excited state and higher lying states (cf. Figure 4 of Paper I¹). Within 500 fs of excitation, the triplet dielectron has reached the ground state and reequilibrated, so a probe pulse would see only the equilibrium spectrum. Panel B displays the ground-state bleach, $\langle -B(t; E) \rangle$; as with the singlet dielectron (and for the same reasons^{19,20}), the bleach looks like the equilibrium spectrum convolved with the instrument response for all times greater than zero. Panel C shows the SE component of the triplet dielectron’s transient spectroscopy, $\langle -S(t; E) \rangle$. The adiabatic eigenstates that lie below the occupied state at time zero have small but nonzero transition dipoles with the occupied state, so there is appreciable SE at all energies below the excitation energy immediately following the excitation. At energies ~ 1.8 eV, there is a strong SE signal for the first few hundred fs

because the initially-occupied excited state has a significant transition dipole with several of the lower-lying states in the excited-state manifold. Because the first excited state rapidly becomes nearly degenerate with the ground state once the first excited state is occupied (see Figure 4 of Paper I¹), the SE signal narrows and red shifts until its greatest magnitude is in the far infrared.

Unlike what we found for the singlet hydrated dielectron, there are few spectral regions that give interesting net signals when the full transient spectroscopy, $\langle\Delta OD\rangle$, of the triplet dielectron is examined. Because of this and the fact that the triplet dielectron is thermodynamically unlikely to exist,²¹ instead of displaying time cuts of the total transient absorption spectrum, we simply describe the features of the total spectrum qualitatively. There is a weak net SE at energies less than ~ 1.8 eV for times less than 250 fs. In addition, there is a slight net transient absorption at energies between 1 and 2 eV, which lasts only a few hundred femtoseconds until the ground state is reoccupied. After the ground state has been repopulated, the total change in absorption vanishes. The main reason that there are few interesting net signals in the transient spectroscopy of the triplet dielectron is that there is a near cancellation between the individual absorption, bleach, and stimulated emission components at most wavelengths; for example, the SE at ~ 1.8 eV is largely canceled by the transient absorption, so there is little net signal in the mid infrared region. Overall, the total pump-probe signal for the triplet dielectron is effectively zero at most wavelengths within simulation error. Moreover, for the few wavelengths at which there is a nonzero net transient bleach or absorption, the net transient signals would overlap with and have the same sign as the signal from the hydrated electron. Thus, there simply would not be enough separation between the pump-probe signals of the triplet dielectron and the (single) hydrated electron to produce a definitive signature for the spectroscopic observation of the triplet hydrated dielectron in the presence of large numbers of hydrated electrons.

IV. Discussion

Since there is no clear pump-probe spectroscopic signature to distinguish triplet dielectrons from hydrated electrons, in this section we focus exclusively on a prediction for detecting the singlet dielectron. We have shown in Figures 2 and 3 that the singlet dielectron possesses an instantaneous bleach to the blue of the exciting wavelength that decays slowly, on a time scale of 700 fs. At ~ 1 eV, there is also a negative net transient absorption signal, which is due to SE, that has a delayed rise and a short (~ 250 fs) lifetime. Near the red edge of the singlet dielectron's ground state absorption spectrum, there is a net transient absorption from the occupied excited state to higher lying states. This net absorption leads us to predict that the transient spectroscopy of singlet dielectrons is significantly different from the transient spectroscopy of hydrated electrons, so that pump-probe spectroscopy could allow singlet dielectrons to be observed directly.

Any experiment to detect hydrated dielectrons will be performed on a sample containing both hydrated electrons and dielectrons, so the spectroscopic signal of the dielectrons would need to be disentangled from the background signal due to electrons. For the conditions of our simulations, in which the singlet dielectron was excited in the near UV, to the blue of the electron's ground state absorption spectrum, Son and co-workers²² have shown experimentally that pumping hydrated electrons at ~ 3.2 eV leads to a transient *bleach* at ~ 1.7 eV, in contrast to the net *absorption* that we predict for singlet

dielectrons at this energy.¹⁰ The experiments also have shown that the bleach recovery time of hydrated electrons is longer (~ 700 fs) when pumped in the UV than when pumped at visible wavelengths.²² The longer bleach recovery time following UV instead of visible excitation is consistent with the picture of hydrated electron relaxation derived from computer simulation:^{23,24} The UV-excited electron is promoted into the continuum, where it either must make several nonadiabatic transitions to reach the vacated ground state, or must carve out a new cavity in a manner similar to what happens for an electron injected directly into water. Thus, it takes longer for the equilibrium absorption spectrum of the hydrated electron to reemerge following UV rather than visible excitation.

Our proposal to observe dielectrons spectroscopically is to produce a population of electrons and dielectrons and perform a pump-probe measurement on this population. We have shown elsewhere that dielectrons are unlikely to be produced in equilibrium.²¹ Thus, the system of electrons and dielectrons may need to be produced as suggested in ref 21 by injecting (either optically or by pulse radiolysis) additional nonequilibrated electrons into water containing already-equilibrated hydrated electrons, which may capture some of the new electrons to form dielectrons. Once this population is formed, the pump-probe experiment proceeds in the usual fashion: The first (pump) pulse is used to excite the mixture of electrons and dielectrons, and the second (probe) pulse is used to probe the effects of the excitation. Excitation at ~ 4 eV will maximize the contribution of dielectrons to the signal because this energy is where the difference in cross section between the hydrated electron and singlet dielectron is the largest. As mentioned above, excitation of hydrated electrons at this energy produces a net transient bleach at ~ 1.7 eV (the maximum of the electron's ground-state absorption),²² but because of their tendency to partially dissociate upon photoexcitation,¹ excitation of singlet dielectrons produces a net transient absorption at this probe wavelength. Thus, our proposed UV-pump/ 1.7 -eV probe experiment is predicted to produce data with a different sign for the two species.¹⁰ This means that it should be straightforward (though not necessarily easy) to monitor the presence of dielectrons, as the relative concentration of electrons and dielectrons is changed by varying the conditions used to produce them.

Our proposed pump-probe experiment not only relies on the net transient spectroscopy of dielectrons and hydrated electrons having opposite signs (bleach for electrons and absorption for dielectrons), but also takes advantage of the fact that dielectrons have a much larger cross section to absorb the UV pump than electrons. The large difference in cross section at ~ 4.0 eV evident in Figure 1 suggests that a sample containing just a few percent dielectrons should give a transient absorption signal from dielectrons with a larger magnitude than the bleach signal from hydrated electrons. Thus, it seems that the main obstacle to observing dielectrons is creating a population of hydrated electrons that contains moderate numbers of dielectrons. As we have suggested elsewhere²¹ and above, such a population might be produced by injecting nonequilibrated electrons into a population of preequilibrated hydrated electrons, some of which would capture one of the injected electrons to form dielectrons. We close by noting that we have not been able to find a way to perform rigorous nonadiabatic calculations of the capture cross section to form hydrated dielectrons,²¹ so an interesting avenue for future research would be to find a way to compute the capture cross section within mixed quantum/classical nonadiabatic molecular dynamics.

Acknowledgment. This work was supported by the NSF under Grant No. CHE-0204776. R.E.L. was a California Nanosystems Institute/Hewlett-Packard Postdoctoral Fellow. B.J.S. is a Camille Dreyfus Teacher-Scholar. We gratefully acknowledge UCLA's Academic Technology Services for the use of its Hoffman Beowulf Cluster.

References and Notes

- (1) Larsen, R. E.; Schwartz, B. J. *J. Phys. Chem. B* **2006**, *110*, 9681.
- (2) Fueki, K. *J. Chem. Phys.* **1969**, *50*, 5381.
- (3) Kaukonen, H.-P.; Barnett, R. N.; Landman, U. *J. Chem. Phys.* **1992**, *97*, 1365.
- (4) Larsen, R. E.; Schwartz, B. J. *J. Chem. Phys.* **2003**, *119*, 7672.
- (5) Larsen, R. E.; Schwartz, B. J. *J. Phys. Chem. B* **2004**, *108*, 11760.
- (6) Garrett, B. C.; Dixon, D. A.; Camaioni, D. M.; Chipman, D. M.; Johnson, M. A.; Jonah, C. D.; Kimmel, G. A.; Miller, J. H.; Rescigno, T. N.; Rosicky, P. J.; Xantheas, S. S.; Colson, S. D.; Laufer, A. H.; Ray, D.; Barbara, P. F.; Bartels, D. M.; Becker, K. H.; Bowen, H.; Bradforth, S. E.; Carmichael, I.; Coe, J. V.; Corrales, L. R.; Cowin, J. P.; Dupuis, M.; Eisenthal, K. B.; Franz, J. A.; Gutowski, M. S.; Jordan, K. D.; Kay, B. D.; LaVerne, J. A.; Lymar, S. V.; Madey, T. E.; McCurdy, C. W.; Meisel, D.; Mukamel, S.; Nilsson, A. R.; Orlando, T. M.; Petrik, N. G.; Pimblott, S. M.; Rustad, J. R.; Schenter, G. K.; Singer, S. J.; Tokmakoff, A.; Wang, L. S.; Wittig, C.; Zwier, T. S. *Chem. Rev.* **2005**, *105*, 355.
- (7) Schmidt, K. J.; Bartels, D. M. *Chem. Phys.* **1995**, *190*, 145.
- (8) Basco, N.; Kenney, G. A.; Walker, D. C. *Chem. Commun.* **1969**, 917. Basco, N.; Kenney-Wallace, G. A.; Vidyarthi, S. K.; Walker, D. C. *Can. J. Chem.* **1972**, *50*, 2059.
- (9) Meisel, D.; Czapski, G.; Matheson, M. S.; Mulac, W. A. *Int. J. Rad. Phys. Chem.* **1975**, *7*, 233.
- (10) With the pseudopotential we use for the electron-water interaction, the absorption spectrum of the hydrated electron is blue shifted by ~ 0.5 eV relative to the experimental spectrum (see ref 19). A similar shift should occur for the hydrated dielectron, so all the simulated energies should be adjusted accordingly when comparing to experiment.
- (11) Allen, M. P.; Tildesley, D. J. *Computer Simulation of Liquids*; Oxford University Press: London, 1992.
- (12) Steinhauser, O. *Mol. Phys.* **1982**, *45*, 335.
- (13) Toukan, K.; Rahman, A. *Phys. Rev. B.* **1985**, *31*, 2643.
- (14) Rosicky, P. J.; Schnitker, J. *J. Phys. Chem.* **1988**, *92*, 4277.
- (15) Prezhdo, O. V.; Rosicky, P. J. *J. Chem. Phys.* **1997**, *107*, 825.
- (16) Schwartz, B. J.; Rosicky, P. J. *J. Chem. Phys.* **1994**, *101*, 6917.
- (17) Sakurai, J. J. *Modern Quantum Mechanics*, revised ed.; Addison-Wesley: Reading, 1994; Chapter 5.
- (18) Nguyen, T.-Q.; Martini, I.; Liu, J.; Schwartz, B. J. *J. Phys. Chem. B* **2000**, *104*, 237.
- (19) Schwartz, B. J.; Rosicky P. J. *Phys. Rev. Lett.* **1994**, *72*, 3282.
- (20) Yu, J.; Berg, M. *J. Phys. Chem.* **1993**, *97*, 1758.
- (21) Larsen, R. E.; Schwartz, B. J. *J. Phys. Chem. B* **2006**, *110*, 1006.
- (22) Son, D. H.; Kambhampati, P.; Kee, T. W.; Barbara, P. F. *Chem. Phys. Lett.* **2001**, *342*, 571.
- (23) Schwartz, B. J.; Rosicky, P. J. *J. Chem. Phys.* **1994**, *101*, 6902.
- (24) Wong, K. F.; Rosicky, P. J. *J. Phys. Chem. A* **2001**, *105*, 2546.